

# Excitons in Molecular Aggregates with Lévy Disorder: Anomalous Localization and Exchange Broadening of Optical Spectra

A. Eisfeld,<sup>1</sup> S. M. Vlaming,<sup>2</sup> V. A. Malyshev,<sup>2</sup> and J. Knoester<sup>2</sup>

<sup>1</sup>*Max Planck Institute for Physics of Complex Systems,  
Nöthnitzer Strasse 38, D-01187 Dresden, Germany*

<sup>2</sup>*Centre for Theoretical Physics and Zernike Institute for Advanced Materials,  
University of Groningen, Nijenborgh 4, 9747 AG Groningen, The Netherlands*

We predict the existence of exchange broadening of optical lineshapes in disordered molecular aggregates and a nonuniversal disorder scaling of the localization characteristics of the collective electronic excitations (excitons). These phenomena occur for heavy-tailed Lévy disorder distributions with divergent second moments - distributions that play a role in many branches of physics. Our results sharply contrast with aggregate models commonly analyzed, where the second moment is finite. They bear a relevance for other types of collective excitations as well.

PACS numbers: 78.30.Ly; 73.20.Mf; 71.35.Aa

During the past decade much work has been devoted to low-dimensional optical materials, such as molecular aggregates, photosynthetic antenna systems, conjugated polymers, and quantum wells and wires. They derive their interest from strong and color-tunable absorption and luminescence properties, fast electromagnetic energy transport, or optical switching [1]. Common to this wide variety of materials is that their properties are rooted in excitonic eigenstates, collective excitations that consist of a linear combination of local excited states. The low-dimensional structure, however, makes these excitations strongly dependent on the presence of disorder in the site energies and (or) the intersite interactions. Disorder localizes the excitons and thereby affects basic properties, such as the optical oscillator strength per state, the absorption linewidth, and the excitation diffusion constant. The standard disorder model considers Gaussian or box-like distributions for the energies or the interactions, which both have a finite second moment.

In this Letter, we show that disorder models with divergent second moments give rise to drastically different results for the exciton states and the collective optical response than the standard ones. To this end, we study molecular aggregates with site disorder taken from distributions that have caught interest in a wide range of physical problems, namely heavy-tailed Lévy distributions [2]. These were introduced originally as "exceptional cases" that do not obey the central limit theorem. However, during the past 20 years it has been recognized that they frequently occur in physics and their divergent second moments give rise to a variety of surprising effects in subfields ranging from statistical physics to optics, plasma physics, and condensed matter physics [3–13]. In the context of the model studied in this Letter, it is of particular interest that molecules embedded in a structurally disordered (glassy) host provide an interesting realization of systems with heavy-tailed disorder. The interactions between the molecule and the multipoles representing the structural disorder of the host give rise to random shifts

of the energy levels of the molecule, which is reflected in the broadening of the absorption line. Indeed, it has been shown experimentally and theoretically that these absorption lines have heavy tails (decaying slower than Lorentzian) [10, 11], with mean and variances obeying Lévy distributions [12, 13].

In previous studies, Lévy statistics applied to a single random variable, such as the displacement of a diffusing particle or excitation energy of a single molecule. Here we present the first study of interacting degrees of freedom that individually obey heavy-tailed Lévy statistics and predict totally new phenomena. More specifically, we show that the model considered has remarkable collective optical properties that differ even qualitatively from the well-studied case of Gaussian disorder [14]. In particular, we find the phenomenon of exchange broadening of the absorption line shape, the counterintuitive appearance of fine structure in the density of states (DOS) and the absorption spectrum with increasing disorder strength, and a nonuniversal disorder scaling of the distribution of exciton localization lengths.

We consider a one-dimensional Frenkel exciton model to describe the optical properties of linear aggregates of dye molecules. In fact, this model is very generic and also is used often to describe the properties of the other optical materials mentioned in the introduction. The model consists of a linear array of two-level molecules with parallel transition dipoles, which interact through dipole-dipole transfer interactions. The optical excitations of this system are described by the eigenstates of the exciton Hamiltonian matrix  $H_{nm} = E_n \delta_{nm} - J(\delta_{m,n+1} + \delta_{m,n-1})$  [14], where for simplicity only nearest-neighbor couplings are considered [15]. The transfer integral  $J > 0$  is assumed to be constant. Disorder is included by taking the site energies  $E_n$  as uncorrelated stochastic variables, drawn from a distribution  $p(E)$ .

Special for our model, as compared to previous studies, is that we consider heavy-tailed Lévy distributions for  $p(E)$ . In particular, we consider the class of symmetric

Lévy distributions with mean zero, given by [16]

$$p(E) = \frac{1}{2\pi} \int_{-\infty}^{\infty} dt e^{iEt} \exp(-|\sigma t|^\alpha). \quad (1)$$

Here,  $\sigma > 0$  and  $0 < \alpha \leq 2$  are called the scale parameter and index of stability, respectively. The former determines the half-width at half maximum (HWHM) of  $p(E)$  and we will hereafter refer to it as the disorder strength, while the latter fixes the asymptotic behavior  $p(E) \sim 1/|E|^{1+\alpha}$  for  $E \gg \sigma$  and  $\alpha < 2$ . The power-law behavior for large  $E$  gives rise to heavy tails in  $p(E)$ , which in turn lead to a divergent second moment.

It should be noted that the average site energy for a disorder realization on the chain,  $\bar{E} = N^{-1} \sum_{n=1}^N E_n$ , also obeys a Lévy distribution, with the same index of stability, but a renormalized disorder strength [16]:

$$\sigma^* = \sigma N^{\frac{1-\alpha}{\alpha}}. \quad (2)$$

This property is referred to as stability of the distribution. For a Gaussian distribution ( $\alpha = 2$ ), Eq. (2) gives the well-known result  $\sigma^* = \sigma/\sqrt{N}$ , which reflects the exchange narrowing effect of the optical line shape of molecular J aggregates [17]: the energy distribution of delocalized excitons is narrower than  $\sigma$ , because they average over the energy fluctuations of the individual sites. By analogy one expects from Eq. (2) that for  $\alpha \leq 1$ , this effect is absent. The Lorentzian case ( $\alpha = 1$ ) is special, as it yields  $\sigma^* = \sigma$ . This case was studied in Refs. [18]; while it does not exhibit exchange narrowing, its main properties still are similar to those for Gaussian disorder. Here, we are particularly interested in distributions with  $\alpha < 1$ , for which  $\sigma^* > \sigma$  (exchange broadening).

We analyzed our model by numerical simulations. We used the algorithm described in Refs. 19 to generate the random energies  $E_n$ , after which the Hamiltonian was diagonalized numerically and the exciton DOS, the absorption spectrum, and the exciton localization lengths  $N_{\text{loc}}$  (inverse participation ratio) were calculated using standard methods [14]. We used chains of 200 sites and averaged over tens of thousands of disorder realizations. As typical examples, the results obtained for  $\alpha = 1/2$  are presented in Figs. 1 - 4.

Figure 1 shows the DOS and the absorption spectrum for various disorder strengths  $\sigma$ . The DOS exhibits a typical one-dimensional (1D) shape, with peaks at the band edges  $E = \pm 2J$  that are smeared by disorder. However, three additional features are visible: one at the band center,  $E = 0$ , and two more at  $E = \pm J$ . The relative importance of these three features strongly depends on  $\sigma$  and  $\alpha$ , revealing a transition from a 1D excitonic DOS to a mostly monomeric DOS with increasing  $\sigma$ . The origin of the extra features, which we found to get more pronounced upon decreasing  $\alpha$ , will be explained below.

The structure in the DOS is also reflected in the absorption spectrum [Fig. 1(b)]. While this spectrum is

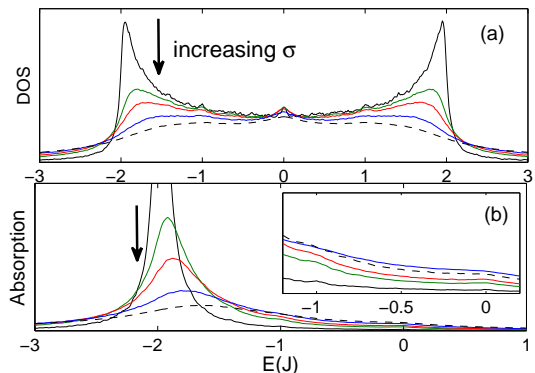


FIG. 1: DOS (a) and absorption spectra (b) for Lévy disorder with  $\alpha = 1/2$  and disorder strengths  $\sigma = 0.01J, 0.1J, 0.2J, 0.5J$ , and  $J$ . The arrows mark the curves in order of increasing  $\sigma$ .

dominated by the intense band edge peak (the J band), characteristic for J aggregates, two much less intense features occur at  $E = -J$  and  $E = 0$ . For Gaussian or Lorentzian disorder these features cannot be discerned. Figure 1(b) also reveals another new effect: with increasing value of  $\sigma$ , the J band shifts to the blue, while for Gaussian disorder a red-shift occurs [14].

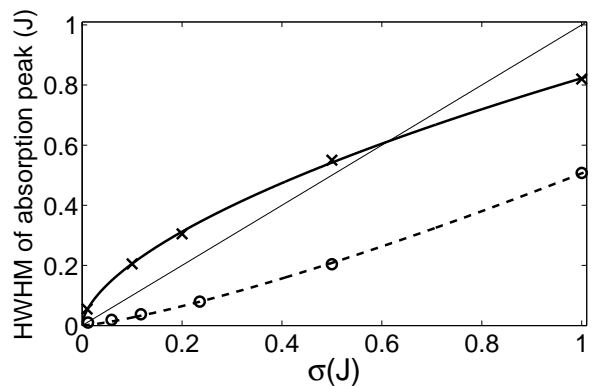


FIG. 2: The HWHM of the absorption spectrum as a function of  $\sigma$  for Lévy disorder with  $\alpha = 1/2$  (crosses) and for Gaussian disorder (circles). The corresponding power law fits are plotted as a solid and a dashed line, respectively. The thin solid line  $\text{HWHM} = \sigma$  is plotted for reference.

Figure 2 gives the HWHM of the absorption band as a function of  $\sigma$ , for  $\alpha = 1/2$  (crosses) and for comparison also for  $\alpha = 2$  (Gaussian; circles). This plot confirms the most fascinating effect of heavy-tailed Lévy distributions, anticipated above, namely the occurrence of exchange broadening: While for Gaussian disorder the HWHM is smaller than the bare disorder  $\sigma$ , for  $\alpha = 1/2$  it is larger (for  $0 < \sigma < 0.6$ ). The best power-law fit to the data reads  $\text{HWHM} = 0.85J (\sigma/J)^{0.60 \pm 0.03}$  (solid line), which

differs strongly from the scaling  $\text{HWHM} \propto J(\sigma/J)^{4/3}$  for the Gaussian case (dashed line) [14]. While the broadening effect qualitatively agrees with Eq. (2), we will see below that the quantitative explanation of the exponent  $0.60 \pm 0.03$  is more subtle.

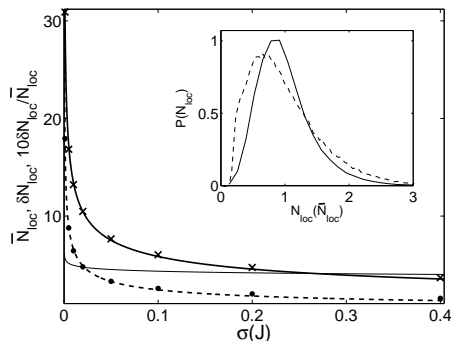


FIG. 3: The average,  $\bar{N}_{\text{loc}}$ , (crosses) and the standard deviation,  $\delta N_{\text{loc}}$ , (dots) of the localization length distribution  $P(N_{\text{loc}})$  as functions of  $\sigma$  for Lévy disorder with  $\alpha = 1/2$ . The thick solid and dashed lines are power-law fits, respectively (see text). The thin solid line gives  $10(\delta N_{\text{loc}}/\bar{N}_{\text{loc}})$ , while the inset shows the localization length distributions for  $\sigma = 0.001J$  (dashed) and for  $\sigma = 0.1J$  (solid).

Finally, Fig. 3 characterizes the distribution  $P(N_{\text{loc}})$  of the localization length of the exciton states that occur in the energy interval  $[-2.1J, -1.9J]$ , i.e., around the lower band edge  $E_b = -2J$ , the region that dominates the optical response. Shown are the numerical data (symbols) and their power-law fits (lines) for the average,  $\bar{N}_{\text{loc}}$ , (crosses and solid line) and the standard deviation,  $\delta N_{\text{loc}}$ , (dots and dashed line) of  $P(N_{\text{loc}})$  as a function of  $\sigma$ . The fits represent the data very well, and read  $\bar{N}_{\text{loc}} = 2.56(J/\sigma)^{0.36}$  and  $\delta N_{\text{loc}} = 0.91(J/\sigma)^{0.43}$ . Thus, the ratio  $\delta N_{\text{loc}}/\bar{N}_{\text{loc}}$  is not constant, implying that, in contrast to Gaussian and Lorentzian disorder [18], Lévy disorder with  $\alpha < 1$  does not lead to a universal function for  $P(N_{\text{loc}})$  in the  $\sigma$ -range considered. This is clearly observed from the inset of Fig. 3, where  $P(N_{\text{loc}})$  is plotted for  $\sigma = 0.001J$  and  $\sigma = 0.1J$ , after scaling the horizontal axis to the average localization length appropriate for the  $\sigma$  value considered. We note that the scaling relations described here, only weakly depend on the choice of the energy interval around  $E_b$ .

The explanation of all phenomena found above, lies in the interplay between two mechanisms for localizing the exciton states around  $E_b$  by heavy-tailed Lévy disorder. For Gaussian disorder only one such mechanism exists, namely localization of states in effective potential wells created by random site energies [20]. The typical localization length  $N^*$  of these states can be obtained from a balance of the energy spacing  $\sim J/N^{*2}$  of two adjacent states within a localization segment and their disorder-induced scattering rate, which scales according

to  $\sigma^*$  given in Eq. (2) with  $N$  replaced by  $N^*$  [21]. Generalizing to the case of Lévy distributions yields

$$N^* = \left( \frac{3\pi^2 J}{\xi_\alpha \sigma} \right)^{\frac{\alpha}{1+\alpha}}, \quad (3)$$

where  $\xi_\alpha$  is a numerical factor of order unity ( $\xi_{1/2} \approx 0.7$ ). For  $\alpha = 1/2$ , this gives  $N^* \propto (J/\sigma)^{1/3}$ . Generally,  $N^*$  is not identical to  $\bar{N}_{\text{loc}}$  because the latter also includes effects of segmentation (see below).

For Gaussian disorder,  $N^*$  is the only length scale relevant to the band edge states and the optical response. In the case of the heavy-tailed Lévy distributions, however, a second localization mechanism - and corresponding length scale - exists. The long tails lead to a high concentration of outliers, i.e., sites with energy  $|E_n| > 2J$ . These fluctuations are so large that the interaction  $J$  cannot overcome them; they therefore break up the chain in segments of length  $N_{\text{seg}}$ , capped by two outliers, which form the maximum intervals over which excitons may delocalize. For decreasing values of  $\alpha$  this effect gets stronger. It is straightforward to show that for  $\alpha \leq 1$  the segment length distribution is exponential, with mean

$$\bar{N}_{\text{seg}} = \frac{\pi}{2\Gamma(\alpha) \sin(\pi\alpha/2)} \left( \frac{2J}{\sigma} \right)^\alpha. \quad (4)$$

$\bar{N}_{\text{seg}}$  is the second length scale in the problem.

The existence of two localization mechanisms is confirmed by Fig. 4, which for  $\alpha = 1/2$  and  $\sigma = 0.1J$  shows a typical realization of the exciton wave functions and energies in the neighborhood of the lower band edge and well below it. Indeed, we observe quite a few outliers, with positions indicated by the vertical dashed lines. Each outlier has a strongly localized  $s$ -like, i.e., without nodes, exciton state (lower panel); not all these states are seen, as several of them have energies outside the plot's range. With regards to the two localization mechanisms, three situations may be distinguished, each of which occurs in Fig. 4.

(i)  $N^* < N_{\text{seg}}$ . This is the situation common for Gaussian disorder. Near the lower band edge one then typically finds doublets of  $s$ - and  $p$ -type states (with no nodes and one node, respectively) roughly localized on the same interval [21]. In Fig. 4 this occurs between  $n = 52$  and  $n = 96$ .

(ii)  $N^* \approx N_{\text{seg}}$ . Here one finds multiplets of three or more states on a single segment, which resemble the states of a disorder-free chain of size  $N_{\text{seg}}$ . In Fig. 4 examples occur between  $n = 1$  and  $n = 31$ , between  $n = 92$  and  $n = 112$ , and between  $n = 164$  and  $n = 200$ .

(iii)  $N^* > N_{\text{seg}}$ . In this case the segmentation strongly confines the excitons and the states within a segment typically get further separated than in the absence of segmentation. If the segments are still relatively large, their lowest  $s$ -like eigenstates contain considerable oscillator strength and occur just above the band edge (e.g.,

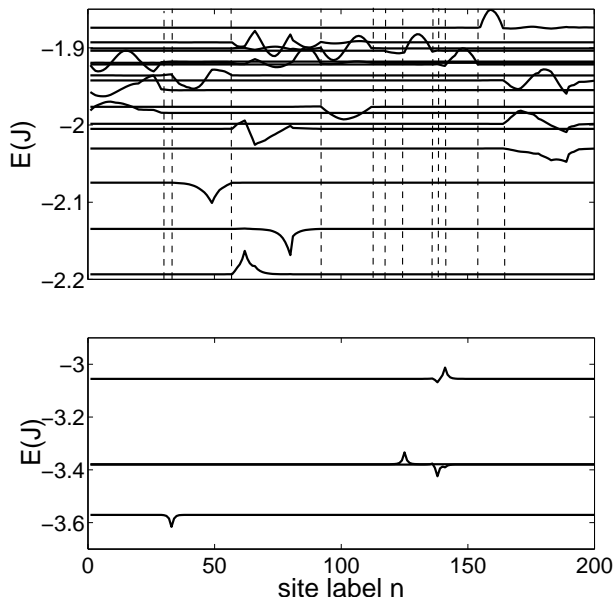


FIG. 4: Exciton wave functions and energies for a typical realization of Lévy disorder with  $\sigma = 0.1J$  and  $\alpha = 1/2$ . The upper panel focuses on energies around the lower band edge; the lower panel displays an energy interval deep in the DOS tail. The dashed vertical lines indicate the positions of outliers in the site energy.

the state between  $n = 154$  and  $n = 164$  in Fig. 4). With increasing value of  $\sigma$ , the segments get shorter and the energy of the  $s$ -like state grows. This explains the blue-shift of the J band found in Fig. 1(b). Also, for growing  $\sigma$ , segments of length 1 and 2 become more likely. These give rise to states with energies distributed around the average monomer and dimer energies,  $E = 0$  and  $E = \pm J$ , respectively, thus explaining the extra features in the DOS and the absorption spectra observed in Fig. 1. Closer scrutiny even reveals features for segments of length 3, 4, etc, but these are weak and overshadowed by the band edge peaks. As is seen in Fig. 1, all these extra features are washed out when  $\sigma$  approaches  $J$ , because they broaden and cannot be distinguished anymore.

Of course, the existence of two localization mechanisms, each with its own length scale, is directly responsible for the observed nonuniversality of the localization length distribution. Moreover, the interplay between both mechanisms also explains the disorder scaling of the exchange broadening of the absorption band. Using Eq. (2) and replacing  $N$  by either  $N^*$  or  $\bar{N}_{\text{seg}}$ , we obtain the contributions to the HWHM from the states localized by the two different mechanisms, respectively. This leads to  $\text{HWHM}^* \propto J(\sigma/J)^{2\alpha/(1+\alpha)}$  and  $\text{HWHM}_{\text{seg}} \propto J(\sigma/J)^\alpha$ . For  $\alpha = 1/2$ , the scaling exponent equals  $2/3$  and  $1/2$ , respectively. Since the numerically obtained exponent equals  $0.60 \pm 0.03$ , we conclude that both scales,  $N^*$  and  $\bar{N}_{\text{seg}}$ , almost equally contribute

to the disorder scaling of the J band width.

In summary, we have shown that heavy-tailed Lévy disorder has dramatic consequences for the optical properties of linear molecular aggregates. Novel effects occur, such as exchange broadening and a nonuniversal scaling of the distribution of exciton localization lengths. We have shown that these effects may all be traced back to the simultaneous occurrence of two different localization mechanisms, each with its own length scale. We expect that the occurrence of two localization length scales has equally dramatic effects on other collective excitations subjected to heavy-tailed disorder.

- 
- [1] For a recent overview, see G.D. Scholes and G. Rumbles, *Nat. Materials* **5**, 683 (2006).
  - [2] P. Lévy, *Bull. Soc. Math. France* **52**, 49 (1924).
  - [3] R. Metzler and J. Klafter, *Phys. Rep.* **339**, 1 (2000).
  - [4] M. F. Shlesinger, G. M. Zaslavski, and J. Klafter, *Nature* **363**, 31 (1993).
  - [5] A. Ott *et al.*, *Phys. Rev. Lett.* **65**, 2201 (1990).
  - [6] I. M. Sokolov, J. Mai, and A. Blumen, *Phys. Rev. Lett.* **79**, 857 (1997).
  - [7] E. Pereira *et al.*, *Phys. Rev. Lett.* **93**, 120201 (2004).
  - [8] P. Barthélemy, J. Bertolotti, and D. S. Wiersma, *Nature* **453**, 495 (2008).
  - [9] A. V. Chechkin, V. Yu. Gonchar, and M. Szydłowski, *Phys. of Plasmas* **9**, 78 (2002).
  - [10] J. Müller, D. Haarer, and B. M. Kharlamov, *Phys. Lett. A* **281**, 64 (2001).
  - [11] B. M. Kharlamov and G. Zumofen, *J. Chem. Phys.* **116**, 5107 (2002).
  - [12] E. Barkai, R. Silbey, and G. Zumofen, *Phys. Rev. Lett.* **84**, 5339 (2000).
  - [13] E. Barkai *et al.*, *Phys. Rev. Lett.* **91**, 075502 (2003).
  - [14] M. Schreiber and Y. Toyozawa, *J. Phys. Soc. Jpn.* **51**, 1528 (1982); H. Fidder, J. Knoester, and D. A. Wiersma, *J. Chem. Phys.* **95**, 7880 (1991).
  - [15] We have checked numerically that accounting for the long-range dipolar coupling between molecules does not quantitatively change the effects found by us, but slightly changes the scaling exponents and prefactors, as well as the values for  $\alpha$  and  $\sigma$  where nonuniversality sets in.
  - [16] W. Feller, *An Introduction to Probability Theory and its Applications*, Wiley, New York (1966).
  - [17] E. W. Knapp, *Chem. Phys.* **85**, 73 (1984).
  - [18] (a) A. Eisfeld and J. S. Briggs, *Phys. Rev. Lett.* **96**, 113003 (2006); (b) S. M. Vlaming, V. A. Malyshev, and J. Knoester, *Phys. Rev. B* **79**, 205121 (2009).
  - [19] J. M. Chambers, C. L. Mallows and B. W. Stuck, *J. Am. Stat. Ass.* **71**, 340 (1976); J. H. McCulloch, *Bull. London Math. Soc.* **28**, 651 (1996).
  - [20] I. M. Lifshits, S. A. Gredeskul, and L. A. Pastur, *Introduction to the Theory of Disordered Systems*, Wiley: New York, 1988.
  - [21] F. Domínguez-Adame and V. A. Malyshev, *Am. J. Phys.* **72** 226 (2004).